

## MISALIGNED JOURNAL BEARINGS

Mart TAMRE

Tallinna Tehnikaülikooli Paraadiiehituse Instituut (Department of Instrument Engineering, Tallinn Technical University), Ehitajate tee 5, EE-0026 Tallinn, Eesti (Estonia)

Presented by R. Kütner

Received 27 February 1995, accepted 1 June 1995

**Abstract.** The paper deals with friction problems of unlubricated or boundary lubricated journal bearings. The aim of the paper is to analyse the misalignment and axial shape effects of rubbing surfaces encountered with unlubricated or boundary lubricated bearings of precise devices. On the one hand, the study is based on the joint analysis of the isothermal contact task of a journal and a bearing bush and journal equilibrium conditions, and on the other hand, on the deformation-adhesion friction model. The results give evidence of minimum friction dissipation energy in a journal bearing characterized by certain surface roughness as well as by characteristic axial shape and position of the surfaces. This enabled us to propose the design concepts by axial profiling of the journal surface to guarantee lower friction losses and higher reliability of the bearing.

**Key words:** journal bearing, boundary lubrication, friction coefficient, misalignment, tilting angle, contact problem, load distribution, roughness, surface profile, seizure.

### 1. INTRODUCTION

Journal bearings are commonly used several at a time to support a shaft. Based on several practical examples, it is evident that the sum of the friction torque calculated by single bearings differs considerably from the measured value of the integral friction torque of the whole bearing system [1]. Geometrical deviations, load asymmetry, and deformations will cause misalignment and local shape defects of rubbing surfaces in the real system. According to the earlier studies, this effect has been regarded as undesirable in the case of unlubricated and boundary lubricated bearings and as removable by the increasing design and manufacturing accuracy. The specificity of the real bearing is in its operation under geometrical constraint determined by the bearing clearance inside which the journal is moving under the effect of a varying frictional equilibrium system [1, 2].

The application of computing methods to analyse journal bearing friction is discussed in [3, 4]. In the earlier approaches, the conformity of rubbing surfaces and parallelism of the body's axes within bearings were mainly assumed in unlubricated and boundary lubricated cases. The bearing behaviour analysis was based mainly upon the assumption of certain pressure distribution independent of shear stress [3, 4]. It is shown in [5, 6] that more realistic solution for bearings to study friction processes in the dry or boundary case is based on evaluating the friction region by the elastorheology theory.

The experimental studies show that actual rubbing surfaces do not commonly exceed 30 per cent of the calculated ones even in a symmetrical loading case [7]. On the other hand, both an increase and a decrease of power loss caused by the change of friction torque tend to have a common trend to a rapid growth up to three times with journal tilting angles  $3 \times 10^{-4} \dots 10^{-3}$  rad [2, 8]. Surface roughness will change the pressure distribution and determine key factors in interacting surfaces deformation-adhesion friction model [4]. Iterative algorithms [9] to consider the effect of asperities on the contact pressure redistribution are applicable to practical approaches. On the other hand, the two layer surface model has proved suitable to simplify solution procedures of complicated contact problems [4]. The idea is related to the deformations of the surface roughness layer within the concentrated contacts as local effects affect only the change of the whole friction region area and therefore the pressure and shear stress distribution. The models presented to study journal and bearing misalignment and shape effects are intended for high sliding speed in circumstances prevailing hydrodynamic lubrication effect [10, 11].

The aim of the paper is to analyse the effects of misalignment and axial shape of rubbing surfaces encountered when using unlubricated or boundary lubricated bearings of precise devices.

## 2. THEORETICAL MODEL

Figure 1 shows the equilibrium of a journal in the bearing system which may be described by the following expressions:

$$\gamma = \arctan \left( \tan \gamma' + \frac{\delta_A (\gamma_A) + \delta_B (\gamma_B)}{l_\Sigma} \right), \quad (1)$$

$$\bar{M}_0 = \frac{\bar{F}_{kA} \cos \beta_A \int \int z p_k (\varphi, z) d\varphi dz}{A \int \int p_k (\varphi, z) d\varphi dz} + \frac{\bar{F}_{kB} \cos \beta_B \int \int z p_k (\varphi, z) d\varphi dz}{B \int \int p_k (\varphi, z) d\varphi dz}, \quad (2)$$



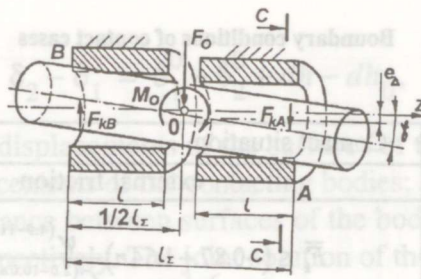


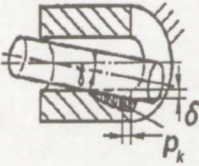
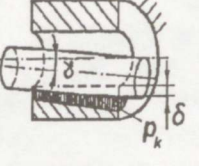
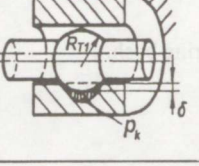
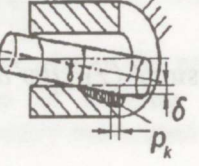
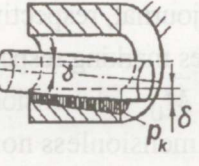
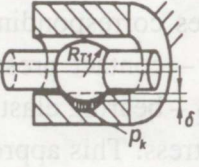
Fig. 1. Misaligned journal bearing, 1 – journal, 2 – bearing bush.

$$\bar{F}_0 = \bar{F}_{kA} + \bar{F}_{kB}, \quad (3)$$

$$M_{FA, B} = \int \int_{A, B} r''(\varphi, z)^2 \tau(\varphi, z) d\varphi' dz, \quad (4)$$

$$F_{kA, B} = \int \int_{A, B} r''(\varphi, z) [p_k(\varphi, z) \cos \varphi'(z) + \tau(\varphi, z) \sin \varphi'(z)] d\varphi' dz, \quad (5)$$

where  $\gamma, \gamma', \gamma_{A, B}$  – general, nominal (without deformations), and actual (average within the contact region) tilting angles of the journal, respectively;  $\delta$  – elastic approach of the contacting bodies;  $A, B$  – indexes marking respective contact regions in the bearing;  $l_{\Sigma}$  – bearing total length;  $M_0$  – dimensionless reduced load moment,  $M_0 = M_0(l_{\Sigma} E_2 r^2)^{-1}$ ;  $F_k$  – dimensionless normal load,  $F_k = F_k(E_2 r^2)^{-1}$ ;  $F_0$  – reduced normal load;  $\beta$  – journal rolling angle;  $z$  – axial co-ordinate;  $\varphi, \varphi'$  angular co-ordinates corresponding to the bearing and the journal centre, respectively;  $p_k$  – contact pressure;  $r, r''$  – nominal and actual (deformed) journal radii;  $E_2$  – bearing elasticity module;  $M_F$  – friction torque;  $\tau$  – tangential contact stress. This approach does not assume any distribution of contact pressures or deformations in advance and is based on the general formula [5]:

| Contact scheme  | Contact situation  |
|---|--|
| external friction   |  |
|    | $\bar{F}_k \leq (-0.87 + 1.64n) \frac{\psi^{(4.9-11.7n)}}{C_0^{(2.0-10.0n)} K_{G1}^{1.5}} \times \left[ \frac{HB}{2^{\nu+1} \Delta^\nu E_2} \left( 1 - \frac{6\tau_n}{HB} \right)^\nu \right]^{(-2.9+11.7n)} \quad (7)$  |
|    | $\bar{F}_k \leq (-4.0 + 9.2n) \frac{\psi^{(1.3-3.4n)} \bar{l}^{(0.14+1.4n)}}{C_0^{(0.8-3.1n)} K_{G1}^{(0.16-0.12n)}} \times \left[ \frac{HB}{2^{\nu+1} \Delta^\nu E_2} \left( 1 - \frac{6\tau_n}{HB} \right)^\nu \right]^{(-0.7+4.1n)} \quad (8)$                                |
|    | $\bar{F}_k \leq (-10.2 + 20.4n) \frac{\psi^{(3.1-7.8n)}}{C_0^{(1.3-6.6n)} K_{G4}^{(0.49+0.08n)}} \times \left[ \frac{HB}{2^{\nu+1} \Delta^\nu E_2} \left( 1 - \frac{6\tau_n}{HB} \right)^\nu \right]^{(-1.7+7.9n)} \quad (9)$  |
| elastic - plastic contact   |  |
|   | $\bar{F}_k = \frac{(3.5n - 1.9) \times 10^3 \psi^{(4.9-11.7n)}}{C_0^{(2.0-10.0n)} (1+f)^{(-7.8+15.0n)} K_{G1}^{1.5}} \times \left[ \left( \frac{HB}{E_2} \right)^5 \left( \frac{1-\mu_2^2}{\Delta^{0.5}} \right)^4 \right]^{(-2.9+11.7n)} \quad (10)$                            |
|  | $\bar{F}_k = \frac{(3.7n - 1.9) \times 10^2 \psi^{(1.3-3.4n)} \bar{l}^{(0.14+1.4n)}}{C_0^{(0.8-3.1n)} (1+f)^{(-1.7+3.1n)} K_{G1}^{(0.16-0.12n)}} \times \left[ \left( \frac{HB}{E_2} \right)^5 \left( \frac{1-\mu_2^2}{\Delta^{0.5}} \right)^4 \right]^{(-0.7+4.1n)} \quad (11)$ |
|  | $\bar{F}_k = \frac{(7.3n - 3.9) \times 10^3 \psi^{(3.1-7.8n)}}{C_0^{(1.3-6.6n)} (1+f)^{(-5.2+10.0n)} K_{G4}^{(0.49+0.08n)}} \times \left[ \left( \frac{HB}{E_2} \right)^5 \left( \frac{1-\mu_2^2}{\Delta^{0.5}} \right)^4 \right]^{(-1.7+7.9n)} \quad (12)$                      |



$$\delta_2 - \delta_1 = \delta_1^0 - \delta_2^0 + dh - dh_0, \quad (6)$$

where  $\delta_1$  and  $\delta_2$  – displacements of the surfaces of the contacting bodies;  $\delta_1^0$  and  $\delta_2^0$  – displacements of the contacting bodies;  $dh$  and  $dh_0$  – thickness of rheological substance between surfaces of the bodies at initial state and at the moment  $t$ , respectively. The joint solution of the formulas (5) and (6) by the finite difference method [1, 6] gives contact pressure distribution within each separate ideally smooth contact region. The situation is treated as an isothermal contact case dealing with temperature rise as a factor changing the elasticity parameters of the bodies within the contact region globally. Figure 2 shows the rebalancing effect of the journal. To take into account the role of surface asperities, the spherical roughness model [4] is applied to each contact element between the nodes. The pressure is assumed constant and known from the first smooth finite difference solution. The aim of the iterative process is to determine additional interference of the contacting bodies caused by linear deformations of the layer. The change of the contact region, considered to be obtained from the interference, allows us to calculate the new pressure distribution between the bodies in the next step. Further calculations produce adjustments to roughness layer deformation and to pressure distribution in each step by turns. In spite of assuming elastic contact of the bodies, the deformation of the asperities can be both elastic or plastic with the model used. Relatively few iterations are needed for the difference of the solutions converging up to 1...2 per cent. As the main result, the numerical solution enabled us to derive approximating expressions to estimate the boundaries of external friction and elastic-plastic transition stage. The Table illustrates the corresponding formulas for a misaligned cylindrical and a barrel journal. In this case,  $n$  and  $C_0$  – the parameters of contacting bodies given in [4];  $\psi$  – relative clearance;  $f$  – friction coefficient;  $K_G$  – coefficient of geometrical deviation [6],  $K_{G1} = (2 \times 10^{-4} + \gamma)$  and  $K_{G4,5} = (5 \times 10^{-5} + R_{T1,2})$ ;  $HB$  – Brinell hardness of softer material;  $\tau_n$  – shear stress;  $\Delta$  – parameter of surface microgeometry,  $\Delta = R_{\max} (r_r b^{1/\nu})^{-1}$ ;  $b$  and  $\nu$  – surface profile parameters;  $R_{\max}$  – maximum height of asperities;  $r_r$  – average top radius of asperities;  $R_T$  – axial curvature radius of journal surface along the axis,  $R_T = R_T r^{-1}$ . Taking into consideration surface roughness, the friction model [4] depending on deformation and adhesion friction components is expressed as

$$f = \tau_0 p_{kc}^{-1} + \beta_k + K_x (\delta_R \Delta b^{1/\nu} R_{\max}^{-1})^{0.5}, \quad (13)$$

where  $\tau_0$  and  $\beta_k$  – the friction parameters;  $p_{kc}$  – apparent contact pressure;  $K_x$  – parameter of asperity deformation [3];  $\delta_R$  – linear deformation of asperities.

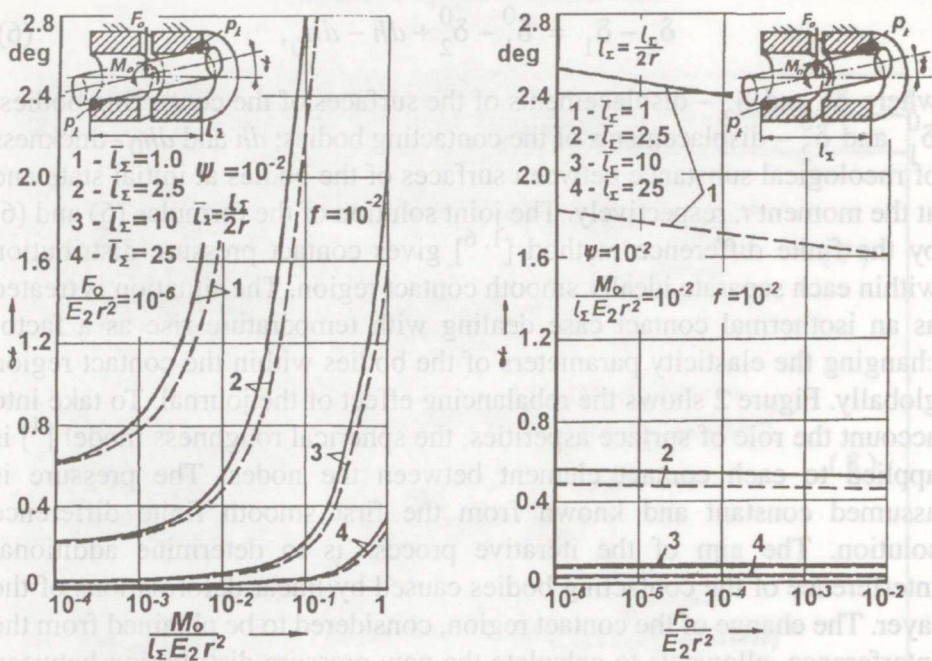


Fig. 2. Effect of load on journal tilting angle, continuous lines – steel - bronze, short dashes – steel - polymer (PA6).

### 3. DISCUSSION

To test misaligned journal bearings without adding any measuring forces that could cause inadequacy of journal behaviour, special test methods and devices were elaborated [1, 12, 13]. A satisfying correlation is observed between experimentally examined bearing seizure situations and numerically calculated limits of external friction changing into internal one (Fig. 3). Bearings made from polymers are less sensitive to position deviations than bearings made from metallic materials. It is typical of  $\gamma$  have little influence on bearing behaviour if  $l$  is shorter than the potential contact region length. The change of apparent contact area  $A_c$  caused by pressure radial redistribution in the case of friction variation is relatively small (if  $f$  changes from 0.05 to 0.5, the area  $A_c$  alters 40 per cent in the case of steel journal and bronze bearing bush). The pressures and deformations change from 0 to maximum value along the contact arc. Because 60 per cent of the contact area supports more than 90 per cent of the radial load, it is reasonable to proceed from the mentioned area to evaluate deformation transition stages. For each contact element between the nodes, we applied the model (13) and calculated the apparent friction coefficient all over the contact area. Then, the theoretical dependence of the resulting friction coefficient on journal tilting angle was estimated. The experimental results indicate that at a certain journal tilting angle [1, 6, 8], a minimum of friction coefficient occurs. In many cases, friction losses are



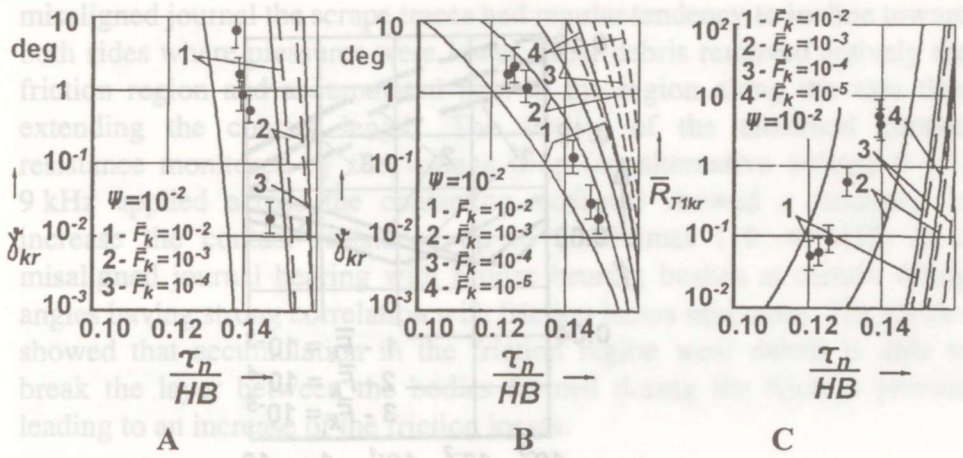


Fig. 3. The critical tilting angle of journal and the critical barrel segment curvature radius of journal vs. relative shear stress, A – contact region is shorter than the bearing bush length, B – contact region length is equal to bearing bush length, C – journal with barrel segments, continuous lines – steel - bronze, short dashes – steel - polymer (PA6) (experiments with bronze bearing bushes,  $F_k = 5 \times 10^{-3}$ ).

increasing with the decrease of the misalignment angle that are characteristic of the elastic deformation stage of asperities although main deformation of the bodies could be plastic or elastic. Experimentally determined friction coefficients are generally higher than calculated quantities though the minimum of the curvature locates nearly at the same value as the numerically calculated ones (Fig. 4). The plastic deformation stage of the asperities is characterised only by the steady state growth of the friction coefficient with the increasing journal tilting angle and with no reduction of the friction coefficient. Numerical solution of the expression  $df/d\gamma = 0$ , regarding journal tilting angle, gives the angle  $\gamma_{\min}$  corresponding to the minimum of friction losses. In the case of the elastic contact of asperities:

$$\gamma_{\min} = \frac{(6.9n - 3.8) \times 10^3 \psi^{(3.7-9.0n)}}{C_0^{(2.1-8.0n)} F_k^{-0.69}} \left[ \frac{K_x \Delta^{0.67} E_2}{\tau_0 (1 - \mu_2^2)^{0.3}} \right]^{(3.5-13.5n)} - 2 \times 10^{-4}, \quad (14)$$

the elastic-plastic transition stage of asperities

$$\gamma_{\min} = \frac{(4.7n - 2.6) \times 10^3 \psi^{(3.7-9.0n)}}{C_0^{(2.1-8.0n)} F_k^{-0.69}} \left[ \frac{\Delta^{0.67} E_2^{2.5}}{HB^{2.5} (1 - \mu_2^2)^2} \right]^{(4.6-18.0n)} - 2 \times 10^{-4}, \quad (15)$$

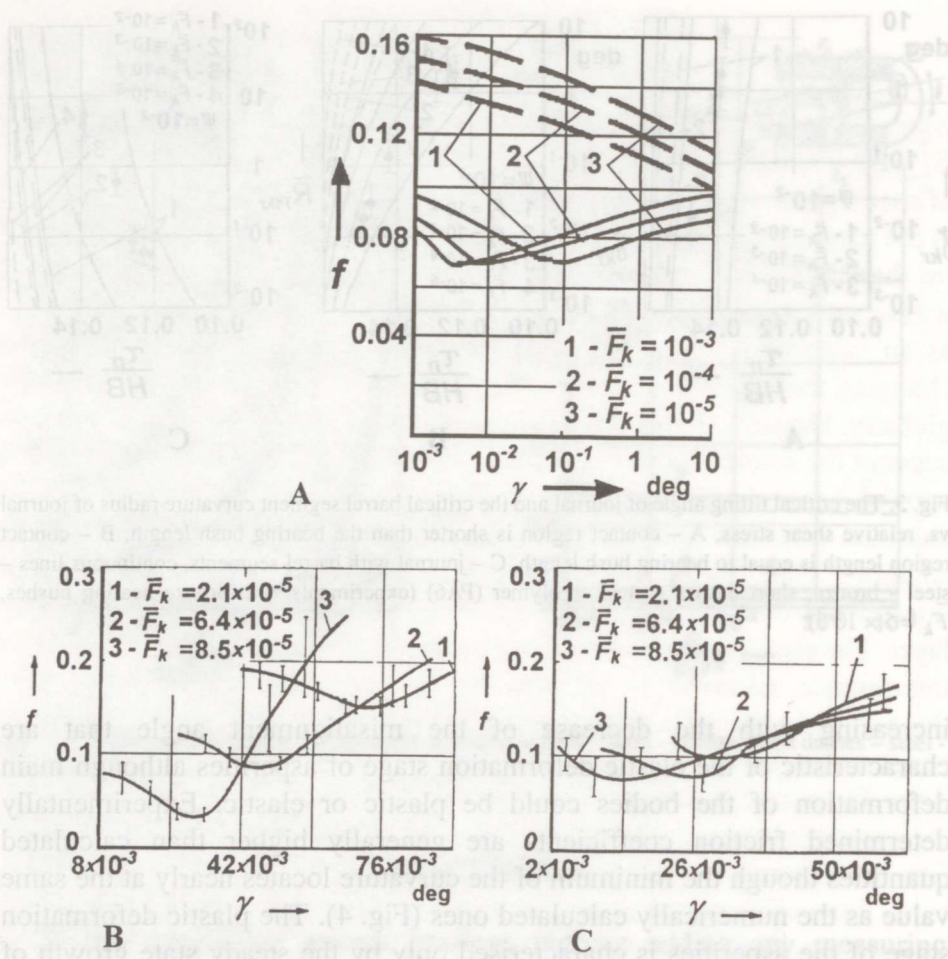


Fig. 4. The effect of journal tilting angle effect on friction coefficient, A - calculated characteristics; B and C - experimental results; B - steel journal - porous bronze bearing bush; C - steel journal - bronze bearing bush (boundary lubrication, lubricant viscosity 0.02 Pa  $\times$  s, velocity 12.6 rad/s,  $r = 1.25$  mm,  $\Delta = 0.001$ ,  $\psi = 0.01$ ).

where  $\mu_2$  - Poisson number of bearing material. It is evident from the analysis and experimental results that conical shape of bodies (taper) has the same effect on the friction as tilting angle [2]. The tilting angle  $\gamma$  must be replaced with half cone angle of the respective surface in (7)...(12) and (14), (15) (resulting deviation is less than 10 per cent) to evaluate the taper effect. In accordance with the experimentally studied higher friction (Fig. 4) we can suppose action of some additional process in the friction region. The process leads to an increase of friction both for an aligned journal and for a high value of the tilting angle. Scrape traces of the wear particles on the surfaces of an aligned bearing were generally parallel to sliding direction with some chaotic character as the studies of the friction surfaces after some working-in period show. There was a tendency to accumulate wear particles in the friction region. On the other hand, with a



misaligned journal the scrape traces had regular tendency to incline toward both sides where pressures were lower. Wear debris removed actively the friction region and accumulated next to the region along the axis thus extending the contact length. The studies of the electrical contact resistance monitored by the voltage drop (an alternative voltage 9 mV, 9 kHz applied across the contacting surfaces) showed a tendency to increase the contact resistance up to 1000 times (10...40 MΩ) in a misaligned journal bearing with bronze bearing bushes at certain tilting angles having strong correlation with friction losses minimum. The studies showed that accumulation in the friction region wear debris is able to break the layer between the bodies formed during the friction process leading to an increase of the friction losses.

#### 4. DESIGN CONCEPTS

Therefore a certain journal misalignment angle must be guaranteed in a bearing system for minimising friction losses. It was also proved that enlargement of the length of the bearing bushes with a misaligned journal does not always lead to an effective solution in the boundary lubrication case [6]. To ensure a certain and extremely small (from 10 to 30 angular minutes) journal misalignment in the bearings is a relatively complicated task because of the tolerances of the bearing elements and variability of journal equilibrium conditions.

Reasonable handling of the axial profile of the rubbing surfaces could give more effective results. Model (13) application for each contact element between the nodes shows that if the normal load does not exceed the value determined by the formulas (9) and (12), the friction coefficient in a bearing with a journal having barrel segments, which constitute specific axial undulation (Fig. 5), is lower than in the case of cylindrical journal when the expression (16) is satisfied. The elastic deformation of asperities is assumed:

$$K_{G4} = \frac{(9.0n - 5.0) \times 10^7 \psi^{(5.8-15.1n)}}{C_0^{(2.7-12.8n)} F_k^{-2.0}} \left[ \frac{K_x \Delta^{0.67} E_2}{\tau_0 (1 - \mu_2^2)^{0.3}} \right]^{(4.3-22.7n)} \quad (16)$$

The test results of the axially profiled bearing in which the boundary conditions (9) and (12) are taken into consideration confirm the assumptions (Fig. 6). Therefore the optimum axial profile radius can be determined from the formula (16). In the case of relative high loads, the number of barrel segments could be increased to a reduced single segment load. Proceeding from the numerical model, the friction coefficient of the axially undulated journal bearing could be evaluated by the approximation expression:

misaligned journal the scrape traces had regular tendency to incline toward both sides where pressures were higher. Debris removed actively the friction region and the contact pressure along the axis thus extending the contact area. The electrical resistance monitoring showed a tendency to increase the contact resistance with increasing journal misalignment. The studies showed that accumulation in the friction zone wear debris is able to break the layer between the bodies formed during the friction process leading to an increase of the friction losses.

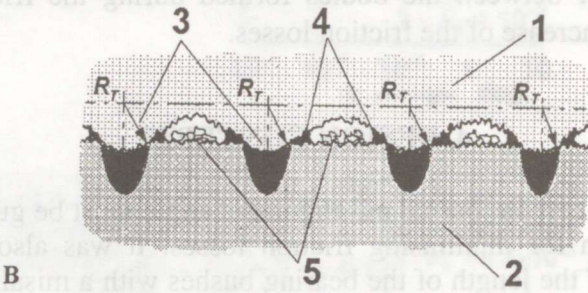


Fig. 5. Axially profiled bearing (with barrel segments), A – scheme; B – axial section, 1 – journal, 2 – bearing bush, 3 – arched segments, 4 – lubrication zones, 5 – grooves for accumulating wear products.

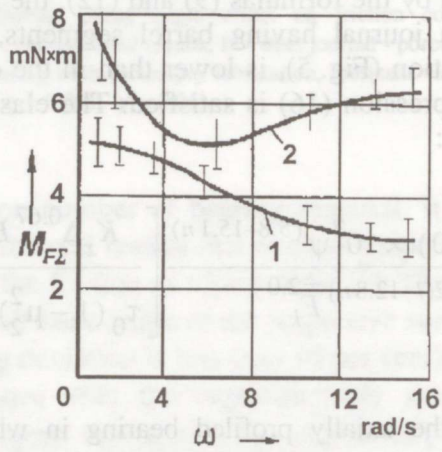


Fig. 6. Friction torque vs. journal velocity, 1 – journal with two barrel segments, 2 – misaligned cylindrical journal, steel journal - bronze bearing bush ( $R_{T1} = 750$  mm,  $F_{kA} = 3.9$  N,  $F_{kB} = 2.3$  N,  $r = 3.65$  mm,  $l = 22$  mm,  $\psi = 0.001$ ,  $R_a = 0.1$   $\mu m$ ).



$$f = \frac{(0.67 + 1.41n) \tau_0 (1 - \mu_2)^{0.67} \Psi^{(0.07-0.40n)} C_0^{0.24}}{E_2 \Delta^{0.3} \bar{F}_k^{(0.27-0.27n)} K_{G4}^{(0.14-0.14n)}} + \beta_k + \frac{(0.51 - 0.30n) K_x (1 - \mu_2)^{0.3} \Delta^{0.3} \bar{F}_k^{(0.27-0.27n)} K_{G4}^{(0.14-0.14n)}}{\Psi^{(0.07-0.40n)} C_0^{0.24}} \quad (17)$$

The experimental results demonstrate that removal of wear particles from the friction region serves as the secondary effect which strengthens the reduction of the friction coefficient if barrel segments are on the journal surface.

## 5. CONCLUSIONS

As a result of the analysis of the behaviour of a bearing system from the point of the tilting journal, the following conclusions can be made. Journal misalignment has a considerable role on the friction process in the case of boundary lubrication. Depending on the journal tilting angle, the characteristic of the friction coefficient has a low point. The reason of this dependence is the effect of deformation-adhesion components of friction. The existence of the low point of friction is related to the elastic deformation of the surface asperities. Friction reduction could be achieved by the axial profiling of the bearing friction surface in the case of boundary lubrication.

## REFERENCES

1. Тамре М. И. Об оптимизации прецизионных радиально-упорных опор скольжения. – Тр. Таллин. техн. ун-та, 1991, 728, 64–77.
2. Ajaots, M. and Tamre, M. Tribocharacteristics of journal bearings of rotating systems with unlocated axis. Research report No. 97. Univ. of Oulu, Department of Mechanical Engineering. – In: Proc. OST-94 Symp. on Machine Design. Tallinn–Oulu, 1994, 62–71.
3. Stolarski, T. A. Tribology in Machine Design. Heinemann Newness, Oxford, 1990.
4. Kragelsky, I. V. and Alisin, V. V. Friction, Wear, Lubrication: Tribology Handbook. Mir, Moscow, 1981–1982.
5. Rymuza, Z. and Kowalski, P. The contact pressure distribution in the friction region of miniature journal bearings. – Wear, 1987, 116, 89–106.
6. Аяотс М. Э., Тамре М. И. Оценка контактных площадей и давлений в парах вал–втулка при наклоненной оси. – Трение и износ, 1993, 14, 2, 334–340.
7. Хандельсман Ю. М., Докучалова В. В. Об оптимальном радиусе оливажа. – Тр. НИИЧаспрома. Часы и часовые механизмы, 1966, 2, 25–29.
8. Ajaots, M. and Tamre, M. Testing the tribological behaviour of a miniature bearing system. – In: Proc. 1st Int. Coll. MICRO-TRIBOLOGY'93, Laliki, Poland, 1993, 18–19.
9. Snidle, R. W. and Evans, H. P. A Direct Method of Elastic Contact Simulation. Report No. 1809, School of Engrg, Univ. of Wales, Cardiff, UK, 1993, 1–17.
10. Basri, S. and Gethin, D. T. Axially profiled circular bearings and their potential application in high speed lubrication. – In: Tribological Design of Machine Elements. Proc. 15th Leeds–Lyon Symp. on Tribology. Leeds, 1988, 211–217.

11. Maspeyrot, P. and Frene, J. Shape defects and misalignment effects in connecting-rod bearings. – In: Tribological Design of Machine Elements. Proc. 15th Leeds–Lyon Symp. on Tribology. Leeds, 1988, 317–322.
12. Аяотс М. Э., Лаанеотс Р. А., Тамре М. И. Емкостный датчик перемещений. Авт. свид. № 1516744 СССР, МКИ G01B7/00. – Б. И., 1989, № 39.
13. Аяотс М. Э., Лаанеотс Р. А., Тамре М. И. Устройство для измерения реакций в опорах привода проигрывателя. Авт. свид. № 1719936 СССР, МКИ G01L3/00, G01P15/02. – Б. И., 1992, № 10.

## KALDTELJEGA LIUGELAAGERDUSED

Mart TAMRE

On käsitletud määrimata või piirmäärimisrežiimil töötavate liugelaagerduste hõõrdeprobleeme. Artikli eesmärk on analüüsida täppisseadmete määrimata või piirmäärimisel töötavates laagerdustes esinevaid hõõrduvate pindade kaldasendi ja aksiaalprofiili efekte.

Töö põhineb ühest küljest laagerduse tapi ja laagripuksi isotermilise elastse kontaktülesande ning tapi tasakaaluülesande koosanalüüsil ja teisest küljest hõõrdeprotsessi molekulaarmehaanilisel mudelil. Saadud tulemused näitavad laagerduses toimuva hõõrdeprotsessi minimaalset dissipatsioonienergiat hõõrduvate pindade kindla pinnakareduse, samuti iseloomuliku pindade aksiaalgeomeetria ja pindade asendi korral. See asjaolu võimaldab välja tuua soovitusel hõõrdekadude vähenemist tagavate ja pikema tööeaga laagerduste loomiseks.

## ОПОРЫ С НАКЛОННОЙ ОСЬЮ

Март ТАМРЕ

Рассмотрены проблемы, связанные с трением опор скольжения, работающих в режиме без смазки или ограниченной смазки. Цель статьи – проанализировать эффекты наклона и аксиального профиля трущихся поверхностей, которые проявляются при эксплуатации опор точных приборов.

Работа основывается, с одной стороны, на совместном анализе изотермического контакта цапфы и подшипника, а также равновесия цапфы, а с другой – на молекулярно-механической модели процесса трения.

Результаты работы показали, что величина минимальной диссипационной энергии фрикционного процесса в опоре зависит не только от шероховатости поверхностей трения, но и от их осевой геометрии и расположения. Поэтому автором предложена концепция проектирования опор с аксиальным профилированием поверхности цапфы, что гарантирует уменьшение энергетических потерь при трении опор и повышает их работоспособность.